Controlling small guanine–nucleotide-exchange factor function through cytoplasmic RNA intramers

Günter Mayer*[†], Michael Blind*[†], Wolfgang Nagel[‡], Thomas Böhm[‡], Thomas Knorr[‡], Catherine L. Jackson[§], Waldemar Kolanus[‡], and Michael Famulok*[¶]

*Kekulé-Institut für Organische Chemie und Biochemie, Rheinische Friedrich-Wilhelms Universität Bonn, Gerhard-Domagk Strasse 1, D-53121 Bonn, Germany; [‡]Laboratorium für Molekulare Biologie-Genzentrum, Ludwig-Maximilians Universität München, Feodor-Lynen Strasse 25, D-81377 Munich, Germany; and §Service de Biochimie et Génétique Moléculaire, Département de Biologie Cellulaire et Moléculaire, Commissariat à l'Energie Atomique/Saclay, F-91191 Gif-sur-Yvette, France

ADP-ribosylation factor (ARF) GTPases and their regulatory proteins have been implicated in the control of diverse biological functions. Two main classes of positive regulatory elements for ARF have been discovered so far: the large Sec7/Gea and the small cytohesin/ARNO families, respectively. These proteins harbor guanine–nucleotide-exchange factor (GEF) activity exerted by the common Sec7 domain. The availability of a specific inhibitor, the fungal metabolite brefeldin A, has enabled documentation of the involvement of the large GEFs in vesicle transport. However, because of the lack of such tools, the biological roles of the small GEFs have remained controversial. Here, we have selected a series of RNA aptamers that specifically recognize the Sec7 domain of cytohesin 1. Some aptamers inhibit guanine–nucleotide exchange on ARF1, thereby preventing ARF activation *in vitro*. Among them, aptamer M69 exhibited unexpected specificity for the small GEFs, because it does not interact with or inhibit the GEF activity of the related Gea2-Sec7 domain, a member of the class of large GEFs. The inhibitory effect demonstrated *in vitro* clearly is observed as well *in vivo*, based on the finding that M69 produces similar results as a dominant-negative, GEF-deficient mutant of cytohesin 1: when expressed in the cytoplasm of T-cells, M69 reduces stimulated adhesion to intercellular adhesion molecule-1 and results in a dramatic reorganization of F-actin distribution. These highly specific cellular effects suggest that the ARF-GEF activity of cytohesin 1 plays an important role in cytoskeletal remodeling events of lymphoid cells.

Cytohesin 1 is a 47-kDa protein comprising an N-terminal coiled-coil domain, a central Sec7 domain, and a C-terminal module consisting of a pleckstrin homology (PH) domain and a polybasic region (1). It interacts with the cytoplasmic tail of the leukocyte-specific $\alpha_L\beta_2$-integrin (LFA-1, CD11a/18) and is thought to regulate adhesion of the extracellular domain of the $\alpha_L\beta_2$-integrin to intercellular adhesion molecule 1 (ICAM-1) (1). Furthermore, cytohesin 1 belongs to the class of small guanine–nucleotide-exchange factors (GEFs) for human ADP-ribosylation factors (ARF) (2–4).

ARFs are Ras-related GTPases that control membrane traffic by functioning as on/off switches depending on whether they are bound to GTP or GDP (5). The conversion of the GDP- to the GTP-bound state is controlled by GEFs that all contain a central Sec7 domain. ARF-GEFs can be subdivided into two major classes: the large (>100-kDa) and small (45- to 50-kDa) GEFs, based on their size, sequence similarities, and function (6, 7). The exchange activity of the large GEFs can be inhibited specifically by the fungal metabolite brefeldin A (BFA). In contrast, the small GEFs, for which inhibitors have not been found until now, are insensitive to BFA (8–10).

Owing to the fact that specific inhibitors for proteins or their subdomains are available only in exceptional cases, most traditional approaches to investigating the function of an individual cellular component rely on observing phenotypes of a cell as a result of altering its genetic information. This commonly is achieved either by knockout technologies or expression/ overexpression of a protein subdomain or a mutant derivative (11). Alternatively, functional information also may be gained by peptide aptamers presented on surface loops (12, 13) or intrabodies (14); however, at least the latter approach bears the inherent problem of maintaining functionality in the reductive milieu of the cytoplasm (15).

Nucleic acid aptamers exhibit highly complex and sophisticated molecular recognition properties and are capable of binding tightly and specifically to a variety of targets (16–19). They are isolated from vast combinatorial nucleic acid libraries by *in vitro* selection and thus can be fine-tuned to function under various conditions. Many aptamers targeted against proteins also are able to interfere with their biological function.

We previously have shown that cytoplasmic expression of aptamers ("intramers") may be used to modulate integrin-dependent adhesion pathways (20). In the present study, we take this approach to another level and use it to gain novel biological information. We show that aptamers can be generated to specifically inhibit small GEF-Sec7 domains. These are the first inhibitors described to target this class of molecules. Furthermore, the aptamers are active in living cells, and, by employing them, we show that the exchange-factor function of cytohesin 1 is involved in remodeling of the actin cytoskeleton. This observation elegantly explains previous findings implicating the Sec7 domain of cytohesin 1 in the control of cell spreading (21).

Methods

Proteins and Peptide. His$_6$-cytohesin 1), His$_6$-C1-Sec7 domain, and His$_6$-PH domain were expressed heterologously in *Escherichia coli*. Purification was achieved by standard Ni^{2+}-nitrilotriacetic acid-chelating affinity chromatography as described (22). His$_6$-Gea2-Sec7 domain and ARNO-Sec7, purified as described (8, 23), were kindly provided by A. Peyroche and S. Robineau (Saclay). His$_6$-cytohesin 1 was coupled directly to CNBr-activated Sepharose according to the manufacturer's instructions (Amersham Pharmacia). The peptide corresponding to the polybasic C domain was purchased from TopLab (Martinsried, Germany). ARF-1 protein was expressed with recombinant vaccinia viruses as carboxyl-terminally fused Ig fusion proteins in COS cells. Purification of Ig chimeras were achieved by immunoprecipitation on protein A-Sepharose (Amersham Pharmacia) as described (4).

BIOCHEMISTRY

Oligonucleotides, Library Construction, and *in Vitro* Selection. The library consisted of 5′-TCTAATACGACTCACTATAGG-GAGAGACAAGCTTGGGTC-N40-AGAAGAGAAAG-AGAAGTTAATTAAGGATCCTCAG-3′ (N40: 40 bases randomized). Purified RNA transcripts were dissolved in selection buffer (3.0 mM $MgCl_2$/147 mM NaCl/2.7 mM KCl/4.3 mM Na_2HPO_4/1.4 mM KH_2PO_4/4 mM DTT/0.8 unit/μl RNasin, pH 7.3) and incubated with His_6-cytohesin 1-Sepharose for 1 h at 37°C. Unbound RNAs were removed with selection buffer, and bound RNAs were eluted with denaturing buffer (30 mM Tris, pH 6.8/20% glycerol/2% SDS/1 M DTT). Eluted RNA was amplified as described (24).

RNA/Protein Interaction Assay. RNA/protein-binding assays were performed by incubating of 1.0 nM 5′ ^{32}P-labeled RNA aptamers with increasing amounts (0.1–500 nM) of cytohesin 1, C1-Sec7, PH, C-domain, or Gea2-Sec7 in selection buffer. RNA/protein complexes were passed through 0.45-μm nitrocellulose filters and washed with 5 ml of wash buffer (3 mM $MgCl_2$/147 mM NaCl/2.7 mM KCl/4.3 mM Na_2HPO_4/1.4 mM KH_2PO_4). Percentages of bound RNA were calculated after PhosphorImager quantification.

GDP/GTP-Exchange Assay. GDP/GTP-exchange assays were performed as described (4) with the following modifications: before the addition of ARF-1, cytohesin 1, C1-Sec7, C2-Sec7, or Gea2-Sec7 (0.65 μM) was incubated with or without individual RNA aptamers at 37°C for 10 min in exchange buffer to allow complex formation. Bound radioactivity was quantified by scintillation counting.

Vaccinia Virus-Based Expression of RNA Aptamers. The M69 aptamer-coding sequence and the control sequence ML1 were inserted via *Xma*I and *Pac*I restriction sites into the transfer T7-RNA expression (TR) vector. Vaccinia virus expression constructs (vTR aptamer) were derived via recombination between the TR vector and wild-type vaccinia virus (WR strain). High-titer virus stocks and double infections with vTR aptamer and a vaccinia virus coding for T7 RNA polymerase (vT7) were generated as described (20, 22).

Adhesion Assays. Jurkat E6 cells were infected with recombinant vaccinia viruses, and cell adhesion to an ICAM-1–Fc fusion protein was measured as described (25) with the following modifications: infections of Jurkat E6 cells were performed for 5 h before adhesion to ICAM-1. Stimulation of cells with phorbol 12-myristate 13-acetate (PMA) at 40 ng/ml was performed at 37°C for 30 min. The results represent an average of three independent experiments, each carried out in triplicate for every value.

Actin Staining. Jurkat E6 cells were infected with recombinant vaccinia viruses as described above. For PMA stimulation, cells were treated with 40 ng/ml PMA for 0.5 h at 37°C 4.5 h after infection. Stimulated and nonstimulated cells were collected by centrifugation and resuspended in Hanks' buffered saline solution (HBSS) before adhesion. Glass slides were coated with a 50-μl drop of 10 μg/ml fibronectin for 1 h at 37°C, and unspecific binding sites were blocked with 2 mg/ml BSA for 2 h, washed twice with HBSS, and subsequently used in the assay. Cells were adhered for 30 min at 37°C to fibronectin-coated glass slides (1.5×10^4 cells per field). Unbound cells were carefully removed with 2×100 μl of HBSS. Adhered cells were fixed with freshly prepared 2% (vol/vol) formaldehyde in PBS at 4°C overnight and blocked with 2% (wt/vol) glycin in PBS for 2 h. Subsequently, cells were permeabilized with 0.2% (vol/vol) Triton X-100 in PBS for 10 min at room temperature. For visualization of actin, cells were incubated with a tetramethylrhodamin-5-

(and -6)-isothiocyanat (TRITC)-labeled phalloidin derivative for 1 h at room temperature. Unbound TRITC-phalloidin was removed with 3×100 μl of PBS. Slides were mounted on mounting medium (Vector Laboratories), and samples were examined by confocal laser microscopy and/or fluorescence microscopy, respectively. Total numbers of cells adhering to fibronectin were similar for all samples (*ca.* 60–70% of total input, data not shown).

Results and Discussion

RNA Aptamers Exhibit Different Modes of Cytohesin 1 Recognition. An initial RNA library of 10^{15} different RNA sequences was screened for binding to recombinant cytohesin 1 immobilized on CNBr-activated Sepharose. After 13 rounds of selection and amplification, the evolved RNA library was cloned and sequenced. The most abundant aptamer M69 occurred at 61% of all clones, indicating that the final pool had been enriched to low complexity. The remaining sequences were represented in low abundance (Fig. 1 *A* and *B*).

Filter-binding assays with subdomain constructs of cytohesin 1 were used to determine dissociation constants (K_d) of some aptamer clones for full-length cytohesin 1 in comparison with the C1-Sec7 domain, the PH domain, and the polybasic C domain (Table 1). To test for specificity with respect to small or large GEF recognition, this analysis also included the Sec7 domain of yeast Gea2 (G2-Sec7), a member of the class of large GEFs (6). M69 binds cytohesin 1 or its Sec7 domain (C1-Sec7) with a K_d of 16 nM (Table 1). No binding to the PH and C domains or to G2-Sec7 was detected, establishing M69 as specific for small GEF recognition. M5 also was a specific Sec7 binder but was not able to discriminate between the two classes of GEFs. With a K_d of 5 nM, M56 turned out as the tightest cytohesin 1 binder; however, this clone recognized individual domains with low affinity or it recognized no domains at all. These data indicate that our selection yielded reagents capable of specifically recognizing Sec7 domains. Moreover, M69 discriminates between the Sec7 domains of small and large GEFs.

Specific Inhibition of Small GEF Activity on ARF1 *in Vitro*. The exchange of high affinity-bound GDP for GTP is required for the activation of ARFs (27). Interaction of GEFs with the ARF-GDP complex lowers its affinity for GDP and, therefore, facilitates its dissociation. GTP then can enter the free guanine–nucleotide-binding site on the ARF-GEF complex, leading to dissociation of the GEF from active ARF-GTP (6).

Having demonstrated that M69 discriminates between the Sec7 domains of large and small GEFs, we were interested in how this specific binding affected the biological activity of various GEFs. We therefore investigated whether this aptamer acts as an inhibitor for ARF-GEF function by employing an *in vitro* guanine–nucleotide-exchange assay (4, 21). As a negative control we used the unselected RNA library, which had no effect on the ARF-GEF activity of all investigated GEFs used in this study (Fig. 2 *A*–*C*). In the presence of a 5-fold molar excess of M69 over protein, however, the exchange activities of cytohesin 1, the C1-Sec7 domain, or the Sec7 domain of cytohesin 2 (C2-Sec7), another member of the small GEF family, were reduced to 40–50% compared with the positive control. In accordance with the binding behavior of M69, no inhibition of G2-Sec7 was observed. The inhibitory activity of M69 occurs in a concentration-dependent manner (Fig. 2*B*). As a positive control, we also assayed the inhibitory effect of BFA on the large GEF G2-Sec7 in comparison with cytohesin 1, C1-Sec7, and C2-Sec7. In accordance with other data (8), a 230-fold molar excess of BFA over protein inhibits G2-Sec7 ARF-GEF function but does not affect the exchange activity of the members of the cytohesin protein family (Fig. 2*D*). Thus, half-maximal inhibition exerted by M69 toward cytohesin 1 is
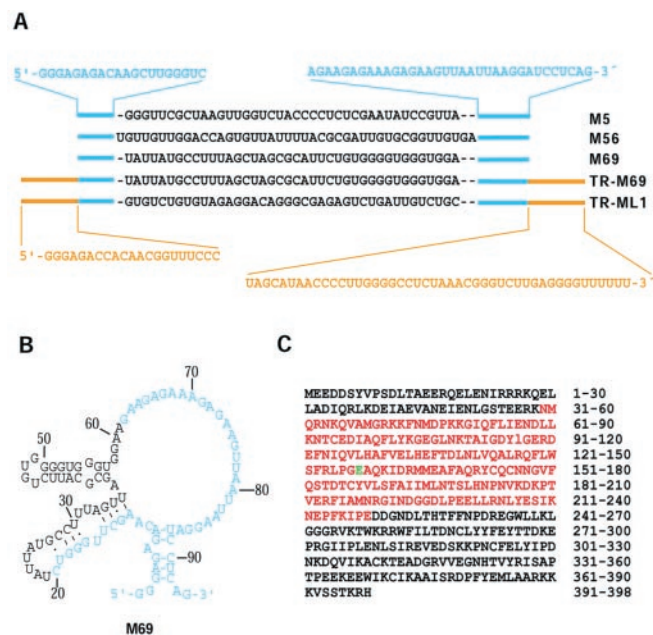
Fig. 1. Sequences of nucleic acids and proteins. (*A*) Nucleic acid sequences of the RNA aptamers M5, M56, M69, TR-M69, and TR-ML1, respectively. Black, initial random sequence; blue, 5′ and 3′ terminal regions for primer annealing; yellow, 5′ and 3′ stem-loop sequences of the TR-expression cassette. (*B*) Secondary structure prediction of M69 proposed by the program MFOLD (26). Blue, constant 5′ and 3′ regions of the RNA aptamer. (*C*) Amino acid sequence of cytohesin 1. Red, C1-Sec7 domain, responsible for M69 binding; green, amino acid E157 residue critical for ARF-GEF activity mutated in cytohesin 1(E157K).

seen at nearly a 50-fold lower concentration as compared with the BFA inhibition of Gea2. These results establish M69 as a potent and long-sought inhibitor for BFA-insensitive GEFs.

T Cell Adhesion to ICAM-1 Is Inhibited by Cytoplasmically Expressed M69. A single point mutant of cytohesin 1, designated as cytohesin 1(E157K), has been reported to be ARF-GEF deficient *in vitro* (4) and to inhibit stimulated Jurkat E6 cell adhesion to ICAM-1 *in vivo* (21). We therefore cloned M69 into a previously developed RNA expression cassette (20) (TR-aptamer, Fig. 1*A*) and investigated whether cytoplasmic expression of M69 affects cytohesin 1-regulated cell adhesion to ICAM-1. Within the new sequence context of the TR aptamer expression cassette, TR-M69 exhibited the same binding behavior and biological activity as the parent M69 aptamer (data not shown).

For high-level expression of TR-M69 in the cytoplasm of Jurkat E6 cells we applied a vaccinia virus-based intramer expression system as described (20). First, recombinant vaccinia

Table 1. K_d of aptamer/protein interaction

Aptamer	K_d, nM*			
	Cytohesin 1	C1-Sec7	PH	G2-Sec7
M5	40.0 ± 8.0	36.0 ± 3.4	480 ± 50	48.0 ± 5.0
M56	5.0 ± 1.0	280 ± 28	150 ± 8.0	>1,000
M69	16.0 ± 0.4	16.0 ± 0.3	NA	NA

Binding of radiolabeled aptamer clones to full-length cytohesin 1 and its subdomains C1-Sec7, PH, and C domain as well as to the large GEF yeast Gea2-Sec7 domain (G2-Sec7) was examined by filter-binding assays. All data were recorded in triplicate measurements. NA, no affinity.
*The C domain peptide NH$_3^+$-CYEMLAARKKKVSSTKRH-COO$^-$ showed no affinity for all three aptamers.

viruses that encode the TR aptamer sequence under the control of the T7 RNA polymerase promoter were generated. The recombinant vaccinia viruses are designated as vTR aptamer. *In vivo* expression of TR-M69 can be induced by double infection of Jurkat E6 cells with the TR-M69-coding virus (vTR-M69) and a second virus coding for T7 RNA polymerase (vT7) (20). After 5 h of double infection, an intramer level of ≈100,000 molecules per cell was obtained (data not shown). All *in vivo* experiments thus were performed at this time point.

Cells were infected with vTR-M69 or a virus that encodes a negative control sequence from the unselected pool, designated as TR-ML1, that neither interacts with cytohesin 1 nor inhibits ARF-GEF function (data not shown). Double-infected Jurkat E6 cells display a considerable background adhesion to ICAM-1, but this nonetheless was superinducible by PMA, a well known promoter of $\alpha_L\beta_2$-integrin-mediated leukocyte adhesion. Intracellular expression of TR-M69 blocks PMA-stimulated adhesion, whereas expression of the control sequence TR-ML1 did not (Fig. 3). Single infections of Jurkat E6 cells with either vT7 or vTR-M69 showed no effect (Fig. 3).

These results demonstrate that M69 specifically inhibits stimulated Jurkat E6 cell adhesion to ICAM-1 *in vivo*. Thus, *in vivo* expression of the anti-C1-Sec7 aptamer M69 results in a similar adhesion deficiency phenotype that also is observed by dominant-negative overexpression of the ARF-GEF-deficient cytohesin 1(E157K) mutant (21). Taken together, these data support the hypothesis that ARF-GEF activity of cytohesin 1 plays a crucial role in $\alpha_L\beta_2$-integrin-mediated leukocyte adhesion.

Expression of TR-M69 or Cytohesin 1(E157K) Affects F-Actin Distribution in Adherent Cells. It was shown recently that expression of the cytohesin 1(E157K) mutant in Jurkat cells resulted in substantially reduced cell spreading (21), a process that is thought to be dependent on actin cytoskeletal-remodeling events. With our highly specific small-GEF inhibitor, intramer TR-M69, and the GEF-deficient cytohesin 1(E157K) mutant
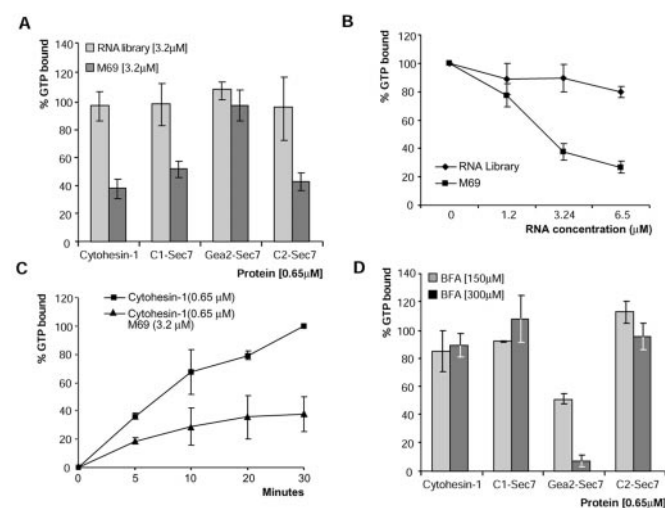
Fig. 2. Inhibition of GDP/GTP exchange on ARF-1 by M69. (*A*) GDP/GTP-exchange activity of cytohesin 1, C1-Sec7, C2-Sec7, and Gea2-Sec7 on ARF-1 in the presence of M69 (solid bars) and unselected RNA library (shaded bars). The amount of bound [γ^{35}-S]GTP after 30 min without RNA was defined as 100%. (*B*) Concentration dependence of inhibition of cytohesin 1-catalyzed GDP/GTP exchange on ARF-1 by M69 (■) and unselected pool (◆). (*C*) Time course of inhibition of cytohesin 1-catalyzed GDP/GTP exchange on ARF-1 by M69 (▲) vs. noninhibited negative control (■). (*D*) GDP/GTP-exchange activity of cytohesin 1, C1-Sec7, C2-Sec7, and Gea2-Sec7 on ARF-1 in the presence of BFA.
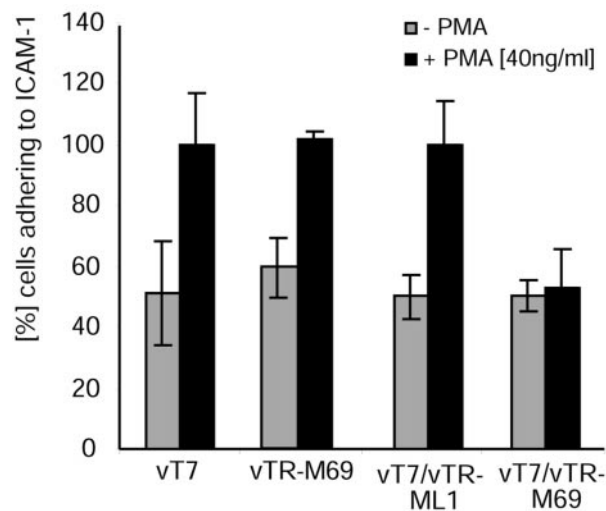
Fig. 3. Adhesion of nonstimulated (shaded bars) and PMA-stimulated (solid bars) Jurkat E6 cells to ICAM-1 as a function of aptamer expression. vT7, single infection with vaccinia viruses expressing T7-RNA polymerase; vTR-M69, single infection with vTR-M69; vT7/vTR-ML1, double infection with vT7 and the nonbinding negative control sequence TR-ML1; vT7/vTR-M69, double infection with vaccinia viruses expressing T7-RNA polymerase (vT7) and TR-M69.

Fig. 4. Actin cytoskeleton staining visualized by fluorescence (*A–D*) and confocal microscopy (*E–H*). (*A*) Single infection with vT7. (*B*) Single infection with vTR-M69. (*C*) Double infection with vT7 and vTR-ML1. (*D*) Double infection with vT7 and vTR-M69. Shown is actin cytoskeleton staining after expression of the constant regions of human IgG antibody CH1 and CH2 (Ig) (*E*), the Ig/cytohesin 1 fusion protein (*F*), the cytohesin 1(E157K) mutant/Ig fusion protein (*G*), and the TR-M69 intramer (*H*).

in hand, we were interested in whether cytoplasmic expression of TR-M69 or dominant-negative overexpression of the mutant affects the organization of the actin cytoskeleton in adherent T cells.

Therefore, we examined the actin distribution in TR-M69 intramer-expressing Jurkat E6 cells adhered to fibronectin by fluorescence microscopy. Fibronectin was chosen as adhesion matrix, because cytohesin 1(E157K) or TR-M69 expression strongly reduce Jurkat cell adhesion to ICAM-1 and, thus, will yield very low numbers of analyzable cells. The result is shown in Fig. 4. Indeed, the intracellular expression of TR-M69 results in dramatic reorganization of the actin cytoskeleton (Fig. 4*D*) compared with cells in which no aptamer is expressed (Fig. 4 *A* and *B*). The expression of the negative control sequence TR-ML1 had no effect on actin cytoskeletal reorganization (Fig. 4*C*). To further support that this intramer-induced cellular phenotype indeed is associated with the inhibition of the ARF-GEF activity of cytohesin 1, we performed an analogous set of experiments employing dominant-negative overexpression of the cytohesin 1(E157K) mutant (Fig. 4 *E–G*). A very similar phenotype, as observed after TR-M69 expression (Fig. 4*H*), is found in cells that express this mutant (Fig. 4*G*). Cells that overexpress either cytohesin 1 or the Ig construct exhibit a normal phenotype (Fig. 4 *E* and *F*). These data strongly suggest that the ARF-GEF activity of cytohesin 1 is implicated in the remodeling of the actin cytoskeleton of T cells. Thereby, our results explain previous findings implicating the Sec7 domain of cytohesin 1 in the control of cell spreading.
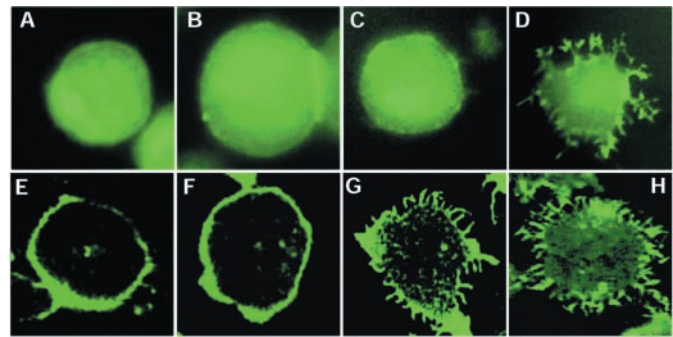
Until now, the expression of dominant-negative mutants has provided powerful means for the dissection of intracellular protein function. Nevertheless, indirect effects are often hard to exclude (28). For example, multidomain proteins might be sequestering numerous factors and, thus, result in complicated changes of the signaling machineries involved. An independent biochemical criterion therefore is highly desirable to assess the validity of data obtained by using dominant-negative mutants (28). We show here that intramers can provide such important validation criteria and are convinced that they will prove to be applicable in various other experimental settings.

We have used an RNA combinatorial approach to obtain a novel class of inhibitors for a family of cytoplasmic regulatory proteins, the small ARF-GEFs, for which no inhibitors have been described until now. The cytoplasmic expression of the RNA aptamer results in the down-regulation of stimulated $\alpha_L\beta_2$-integrin-mediated T cell adhesion to ICAM-1. Furthermore, it induces reorganization events of the actin cytoskeleton that are indistinguishable from those observed after dominant-negative overexpression of the GEF-deficient cytohesin 1(E157K) mutant, thereby linking the GEF activity of cytohesin 1 to these cellular effects.

The power of combinatorial selection combined with the ability to functionally express a resulting inhibitor in the relevant compartment of a living cell represents a new paradigm for gaining information about individual proteins or subdomains in their natural expression context.

1. Kolanus, W. & Zeitlmann, L. (1998) *Curr. Top. Microbiol. Immunol.* **231,** 33–49.
2. Meacci, E., Tsai, S. C., Adamik, R., Moss, J. & Vaughan, M. (1997) *Proc. Natl. Acad. Sci. USA* **94,** 1745–1748.
3. Pacheco-Rodriguez, G., Meacci, E., Vitale, N., Moss, J. & Vaughan, M. (1998) *J. Biol. Chem.* **273,** 26543–26548.
4. Knorr, T., Nagel, W. & Kolanus, W. (2000) *Eur. J. Biochem.* **267,** 3784–3791.
5. Boguski, M. S. & McCormick, F. (1993) *Nature (London)* **366,** 643–654.
6. Jackson, C. L. & Casanova, J. E. (2000) *Trends Cell Biol.* **10,** 60–67.
7. Donaldson, J. G. & Jackson, C. L. (2000) *Curr. Opin. Cell Biol.* **12,** 475–482.
8. Peyroche, A., Antonny, B., Robineau, S., Acker, J., Cherfils, J. & Jackson, C. L. (1999) *Mol. Cell.* **3,** 275–285.
9. Sata, M., Moss, J. & Vaughan, M. (1999) *Proc. Natl. Acad. Sci. USA* **96,** 2752–2757.
10. Chardin, P. & McCormick, F. (1999) *Cell* **97,** 153–155.
11. Brent, R. (2000) *Cell* **100,** 169–183.
12. Colas, P., Cohen, B., Jessen, T., Grishina, I., McCoy, J. & Brent, R. (1996) *Nature (London)* **380,** 548–550.
13. Norman, T. C., Smith, D. L., Sorger, P. K., Drees, B. L., O'Rourke, S. M., Hughes, T. R., Roberts, C. J., Friend, S. H., Fields, S. & Murray, A. W. (1999) *Science* **285,** 591–595.
14. Rondon, I. J. & Marasco, W. A. (1997) *Annu. Rev. Microbiol.* **51,** 257–283.
15. Proba, K., Worn, A., Honegger, A. & Plückthun, A. (1998) *J. Mol. Biol.* **275,** 245–253.
16. Ellington, A. D. & Szostak, J. W. (1990) *Nature (London)* **346,** 818–822.

17. Tuerk, C. & Gold, L. (1990) *Science* **249,** 505–510.
18. Famulok, M. & Mayer, G. (1999) *Curr. Top. Microbiol. Immunol.* **243,** 123–136.
19. Famulok, M., Mayer, G. & Blind, M. (2000) *Acc. Chem. Res.* **33,** 591–599.
20. Blind, M., Kolanus, W. & Famulok, M. (1999) *Proc. Natl. Acad. Sci. USA* **96,** 3606–3610.
21. Geiger, C., Nagel, W., Boehm, T., van Kooyk, Y., Figdor, C. G., Kremmer, E., Hogg, N., Zeitlmann, L., Dierks, H., Weber, K. S., *et al.* (2000) *EMBO J.* **19,** 2525–2536.
22. Kolanus, W., Nagel, W., Schiller, B., Zeitlmann, L., Godar, S., Stockinger, H. & Seed, B. (1996) *Cell* **86,** 233–242.
23. Goldberg, J. (1998) *Cell* **95,** 237–248.
24. Klug, S. J., Huttenhofer, A., Kromayer, M. & Famulok, M. (1997) *Proc. Natl. Acad. Sci. USA* **94,** 6676–6681.
25. Nagel, W., Zeitlmann, L., Schilcher, P., Geiger, C., Kolanus, J. & Kolanus, W. (1998) *J. Biol. Chem.* **273,** 14853–14861.
26. Mathews, D. H., Sabina, J., Zuker, M. & Turner, D. H. (1999) *J. Mol. Biol.* **288,** 911–940.
27. Bourne, H. R., Sanders, D. A. & McCormick, F. (1991) *Nature (London)* **349,** 117–127.
28. Feig, L. A. (1999) *Nat. Cell. Biol.* **1,** E25–E27.

BIOCHEMISTRY